

# Wideband 360 degrees microwave photonic phase shifter based on slow light in semiconductor optical amplifiers

**Xue, Weiqi; Sales, Salvador; Capmany, Jose; Mørk, Jesper**

*Published in:*
Optics Express

*Link to article, DOI:*
10.1364/OE.18.006156

*Publication date:*
2010

*Document Version*
Publisher's PDF, also known as Version of record

# Wideband 360° microwave photonic phase shifter based on slow light in semiconductor optical amplifiers

**Weiqi Xue,[1,*] Salvador Sales,[2] José Capmany,[2] and Jesper Mørk[1]**

[1]*DTU Fotonik, Department of Photonics Engineering, Technical University of Denmark, Build. 343, DK-2800 Kongens Lyngby, Denmark*

[2]*Institute of Telecommunications and Multimedia Applications, Universidad Politécnica de Valencia, Camino de Vera s/n, 46020 Valencia, Spain*

**wexu@fotonik.dtu.dk*

**Abstract:** In this work we demonstrate for the first time, to the best of our knowledge, a continuously tunable 360° microwave phase shifter spanning a microwave bandwidth of several tens of GHz (up to 40 GHz) by slow light effects. The proposed device exploits the phenomenon of coherent population oscillations, enhanced by optical filtering, in combination with a regeneration stage realized by four-wave mixing effects. This combination provides scalability: three hybrid stages are demonstrated but the technology allows an all-integrated device. The microwave operation frequency limitations of the suggested technique, dictated by the underlying physics, are also analyzed.



**OCIS codes:** (230.4320) Nonlinear optical devices; (190.4380) Nonlinear Optics; (140.4480) Optical amplifiers.

## References and links

1. L. V. Hau, S. E. Harris, Z. Dutton, and C. H. Behroozi, "Light speed reduction to 17 metres per second in an ultracold atomic gas," Nature **397**(6720), 594–598 (1999).
2. M. S. Bigelow, N. N. Lepeshkin, and R. W. Boyd, "Observation of ultraslow light propagation in a ruby crystal at room temperature," Phys. Rev. Lett. **90**(11), 113903 (2003).
3. C. J. Chang-Hasnain, and S. L. Chuang, "Slow and fast light in semiconductor quantum-well and quantum-dot devices," J. Lightwave Technol. **24**(12), 4642–4654 (2006).
4. J. Mørk, F. Öhman, M. van der Poel, Y. Chen, P. Lunnemann, and K. Yvind, "Slow and fast light: controlling the speed of light using semiconductor waveguides," Laser Photon Rev. **3**(1-2), 30–44 (2009).
5. Y. A. Vlasov, M. O'Boyle, H. F. Hamann, and S. J. McNab, "Active control of slow light on a chip with photonic crystal waveguides," Nature **438**(7064), 65–69 (2005).
6. T. Baba, "Slow light in photonic crystals," Nat. Photonics **2**(8), 465–473 (2008).
7. Y. Okawachi, M. S. Bigelow, J. E. Sharping, Z. Zhu, A. Schweinsberg, D. J. Gauthier, R. W. Boyd, and A. L. Gaeta, "Tunable all-optical delays via Brillouin slow light in an optical fiber," Phys. Rev. Lett. **94**(15), 153902 (2005).
8. D. Dahan, and G. Eisenstein, "Tunable all optical delay via slow and fast light propagation in a Raman assisted fiber optical parametric amplifier: a route to all optical buffering," Opt. Express **13**(16), 6234–6249 (2005).
9. L. Thévenaz, "Slow and fast light in optical fibers," Nat. Photonics **2**(8), 474–481 (2008).
10. J. T. Mok, and B. J. Eggleton, "Photonics: expect more delays," Nature **433**(7028), 811–812 (2005).
11. T. F. Krauss, "Why do we need slow light?" Nat. Photonics **2**(8), 448–450 (2008).
12. J. Mørk, R. Kjær, M. van der Poel, and K. Yvind, "Slow light in a semiconductor waveguide at gigahertz frequencies," Opt. Express **13**(20), 8136–8145 (2005).
13. S. Chang, P. K. Kondratko, H. Su, and S. L. Chuang, "Slow light based on coherent population oscillation in quantum dots at room temperature," IEEE J. Quantum Electron. **43**(2), 196–205 (2007).
14. A. V. Uskov, F. G. Sedgwick, and C. J. Chang-Hasnain, "Delay limit of slow light in semiconductor optical amplifiers," IEEE Photon. Technol. Lett. **18**(6), 731–733 (2006).
15. W. Xue, Y. Chen, F. Öhman, S. Sales, and J. Mørk, "Enhancing light slow-down in semiconductor optical amplifiers by optical filtering," Opt. Lett. **33**(10), 1084–1086 (2008).
16. J. Capmany, and D. Novak, "Microwave photonics combines two words," Nat. Photonics **1**(6), 319–330 (2007).
17. R. Jakoby, P. Scheele, S. Müller, and C. Weil, "Nonlinear dielectrics for tunable microwave components." 15th International Conference on Microwaves, Radar and Wireless Communications, MIKON-2004, **2**, 369–378 (2004).

#122608 - $15.00 USD Received 12 Jan 2010; revised 22 Feb 2010; accepted 9 Mar 2010; published 11 Mar 2010

18. C. Weil, S. Müller, P. Scheele, Y. Kryvoshapka, G. Lüssem, P. Best, and R. Jakoby, "Ferroelectric- and liquid Crystal tunable microwave phase-shifters," 33rd European Microwave Conference, Munich, Germany, **3**, 1431–1434, (2003).
19. P. Wang, C. Y. Tan, Y. G. Ma, W. N. Cheng, and C. K. Ong, "Planar tunable high-temperature superconductor microwave broadband phase shifter with patterned ferroelectric thin film," Supercond. Sci. Technol. **20**(1), 77–80 (2007).
20. N. S. Barker, and G. M. Reveis, "Distributed MEMS true-time delay phase shifters and wide-band switches," IEEE Trans. Microw. Theory Tech. **46**(11), 1881–1890 (1998).
21. G. McFeetors, and M. Okoniewski, "Distributed MEMS analog phase shifter with enhanced tuning," IEEE Microw.Wirel. Comp. Lett. **16**(1), 34–36 (2006).
22. T. Kim, D. Woo, C. Lee, and K. W. Kim, "A new 40 GHz analog phase shifter using phase-locked loops," 35th European Microwave Conference, Paris, France, **2**, (2005).
23. P. F. McManamon, T. A. Dorschner, D. L. Corkum, L. J. Friedman, D. S. Hobbs, M. Holz, S. Liberman, H. Q. Nguyen, D. P. Resler, R. C. Sharp, and E. A. Watson, "Optical phased array technology," Proc. IEEE **84**(2), 268–298 (1996).
24. J. Capmany, B. Ortega, D. Pastor, and S. Sales, "Discrete-time optical Processing of microwave signals," J. Lightwave Technol. **23**(2), 702–723 (2005).
25. K. Matsumoto, M. Izutsu, and T. Sueta, "Microwave phase shifter using optical waveguide structure," J. Lightwave Technol. **9**(11), 1523–1527 (1991).
26. Y. Yu, and J. P. Yao, "A tunable microwave photonic filter with a complex coefficient using an optical RF phase shifter," IEEE Photon. Technol. Lett. **19**, 1472–1474 (2007).
27. W. Xue, S. Sales, J. Capmany, and J. Mørk, "Microwave phase shifter with controllable power response based on slow- and fast-light effects in semiconductor optical amplifiers," Opt. Lett. **34**(7), 929–931 (2009).
28. W. Xue, Y. Chen, F. Öhman, and J. Mørk, "The role of input chirp on phase shifters based on slow and fast light effects in semiconductor optical amplifiers," Opt. Express **17**(3), 1404–1413 (2009).
29. M. Nielsen, and J. Mørk, "Increasing the modulation bandwidth of semiconductor-optical-amplifier-based switches by using optical filtering," J. Opt. Soc. Am. B **21**, 1606–1619 (2004).
30. B. Dagens, A. Markus, J. X. Chen, J.-G. Provost, D. Make, O. Le Gouezigou, J. Landreau, A. Fiore, and B. Thedrez, "Giant linewidth enhancement factor and purely frequency modulated emission from quantum dot laser," Electron. Lett. **41**(6), 323–324 (2005).
31. W. Xue, S. Sales, J. Capmany and J. Mørk, "Experimental Demonstration of 360° Tunable RF Phase Shift using Slow and Fast Light Effects," in Slow and Fast Light, OSA Technical Digest (CD) (Optical Society of America, 2009), paper SMB6.

## 1. Introduction

The possibility of controlling the speed of light has stimulated significant research efforts [1–9] in the past several years due to intriguing physics as well as a number of promising applications [10,11]. In particular, slow and fast light effects in semiconductor waveguides [12–15] have been extensively researched because of distinct advantages in terms of small size, prospect for integration, operation at room temperature, and low power consumption. One of the exciting motivations is their potential applications in the field of microwave photonics [16]. Microwave photonics exploits the inherent properties of photonic devices to enable complex signal processing functionalities in the microwave and millimeter-wave band that are difficult or impossible to implement directly in the radiofrequency domain. A paradigmatic example is that of tunable microwave and millimeter-wave components, in particular, phase shifters are needed as key components in many communication circuits and applications based on phased antenna arrays (narrowband applications) and in future reconfigurable radiofrequency front-ends [17]. The large size, high cost and limited dynamic range of ferrite-based phase shifters, that are dominant in antenna arrays, prevent the widespread use of phased-arrays in public communications. The trend of these and other emergent applications involves a strong demand for integrated and compact devices featuring both high tunablitiy and low insertion losses.

For a microwave phase shifter, the following parameters are very important: size, absolute magnitude of phase shift $\Delta\Phi$ in degrees, working frequency range, operation voltage, and response time. Ferroelectric materials [18] provide moderate phase shift (20-38 GHz with 360° achieved only at 38 GHz), and very fast response time (<1 ns). Its operation voltage ranges from several tens of volts to 100 volts. Superconductor devices [19] have limited phase shifts (up to 20°) over a bandwidth of 7-11 GHz and require considerable operation voltage ~200 volts. Nematic liquid crystals [18] can provide ~270° phase shifts at 20 GHz with the operation voltage on the order of 30 volts, but the response time is on the order of several

#122608 - $15.00 USD Received 12 Jan 2010; revised 22 Feb 2010; accepted 9 Mar 2010; published 11 Mar 2010

microseconds; The phase shifter based on MEMS [20,21] either leads to inherently digital phase change with discrete states, or requires long response time (>5 μs). Implementations based on electronic phase-locked loops [22] can achieve 640° phase shifts at 40 GHz, but require complex designs and have a limited bandwidth (~40 MHz). Since current technologies thus do not meet the application requirements, especially in the millimeter-wave bands, it is natural to consider the development of compact, continuously tunable microwave phase shifters by optical methods as an alternative with additional advantages such as electromagnetic immunity and light weight [23,24]. A number of different physical schemes have been investigated [25–27]. Among these, slow and fast light effects in semiconductor optical amplifiers (SOAs) appear more promising because they can provide both very fast (on the order of several hundreds of picoseconds) electrically and optically controlled tunability over a microwave bandwidth of several tens of GHz in a compact device with a control voltage of a few volts [27].

The physical effects to induce light slow-down or speed-up in semiconductor waveguides are coherent population oscillations (CPO) [2–4]. Generally, the microwave signal at the frequency of $\Omega$ is intensity modulated onto a continuous-wave laser. Therefore, the input optical signal in the optical frequency domain is composed of a strong carrier, the pump, and two weak sidebands, the probes. Due to the intensity modulation, the populations oscillate at the beat frequency $\Omega$ between the pump and probes [12]. For an SOA, the gain and refractive index are modulated in time and the corresponding temporal gratings subsequently scatter the probe fields and alter their amplitude and phase. The resulting detuning dependence of the probe phase, described in terms of an effective index, leads to a change in the group velocity experienced by the probe signals. After propagating through the SOA, the envelope of the optical signal will thus be delayed or advanced, corresponding to slow or fast light, which can be expressed and measured as a microwave phase shift.

It can be shown that the contribution of the temporal index grating leads to an anti-symmetric detuning dependence of the probe phase, and upon detection of both sidebands this effect cancels out and the phase change is governed solely by the gain dynamics [12]. In this regime the slow/fast light effects can thus be described as the effect of absorption/gain saturation and will be limited in frequency and magnitude by the carrier recovery of the electro-absorbers/SOAs. Recently, we showed that the dynamics of the refractive index can be used to advantage by introducing optical filtering and obtained a 150° phase shift at the microwave frequency of 19 GHz [15]. The principle is illustrated as the 1st stage in Fig. 1a. An optical notch filter is employed, after the SOA, to block the red-shifted sideband, as the optical spectrum shows in the inset (3). These optical filtering enhanced slow light effects can be illustrated by considering the evolution of the slowly varying complex sideband amplitudes in a polar representation, see Fig. 1b. The optical phase of the strong carrier is chosen as the reference, as shown by the green arrows. At the input, the electrical fields of both the strong carrier and sidebands can be taken as real (Fig. 1b (1)). Before optical filtering, the resulting microwave phase shift of the modulated signal has contributions from both sidebands (black shaded area in Fig. 1b (2)), corresponding to a phase advance of a few tens degrees at a few GHz [14]. Now, when blocking the red-shifted sideband after the SOA, the cancellation of the phase of the two sidebands is avoided and the refractive index dynamics, quantified by the linewidth enhancement factor $\alpha$, contributes a large positive phase shift to the blue-shifted sideband. This phase shift dominates the total phase shift of the microwave modulation (blue shaded area in Fig. 1b (3)) [15], thus corresponding to slow light.

#122608 - $15.00 USD Received 12 Jan 2010; revised 22 Feb 2010; accepted 9 Mar 2010; published 11 Mar 2010

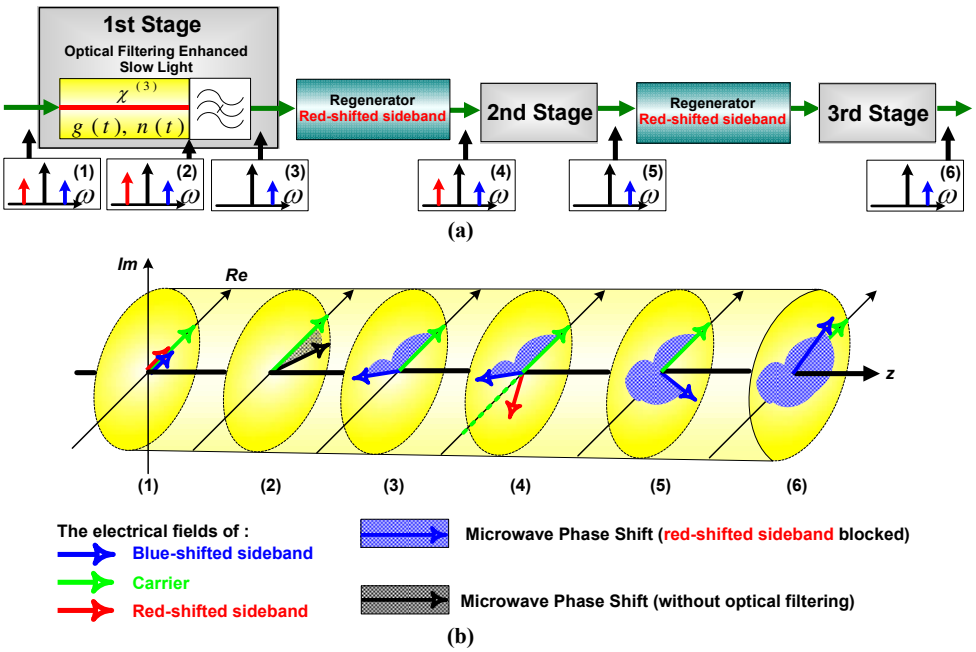


Fig. 1. Configuration of a 360° microwave photonic phase shifter. (a) Simplified diagram showing the cascading of stages of phase shifters followed by regenerators. Both functionalities can be implemented in active waveguides by using the effects of population oscillations and wave mixing. (b) Illustrations of the evolution of the complex amplitudes of the sidebands in a polar representation.

## 2. Achievement of 360° phase shifts

Due to saturation effects, increasing the absolute phase shift by simply increasing the length of the SOA or cascading several SOAs is not possible [28]. To enable the cascading of several stages of optical filtering enhanced slow light elements, in order to achieve an accumulated microwave phase shift of 360°, we introduce a regenerator between two stages, with the purpose of restoring the double sideband characteristic of the original signal, cf. Fig. 1a (4) and Fig. 1b (4). By adding the second phase shift stage, the modulated optical signal will experience a similar effect as in the first stage (Fig. 1b (5)). When a third stage is incorporated we therefore achieve a total of more than 360° tunable microwave phase delay over a microwave bandwidth of several tens of GHz, Fig. 1b (6). The regeneration of the sideband can be achieved using four-wave mixing effects, where the fast build-up of the conjugate signal at the mirror frequency is a well-known effect that can be achieved with high-efficiency in active semiconductor waveguides. Therefore, both the phase shift and the regeneration can be accomplished using the same technology of active semiconductor waveguides.

### *2.1 Theoretical simulations*

The contour plots in Fig. 2 show the calculated microwave phase shifts when the injection currents ($I_1$, $I_2$, $I_3$) of the three SOAs in three stages are increased, one by one, from the transparent current 20 mA to the maximum value 300 mA. The two regeneration SOAs are biased at a fixed current to get the maximum regeneration efficiency. For the conventional case without optical filtering, as shown in Fig. 2a, the CPO effects in an SOA induce the fast light and thus give a total −180° microwave phase shift at 5 GHz. When the red-shifted sidebands are blocked by optical filtering, Fig. 2b demonstrates >360° microwave phase shifts between 6 GHz and 40 GHz. The simulation results are capable of theoretically demonstrating the scalability of the optical filtering enhanced light slow-down and the possibility of achieving a continuously tunable 360° microwave phase shift over a bandwidth of several tens

#122608 - $15.00 USD Received 12 Jan 2010; revised 22 Feb 2010; accepted 9 Mar 2010; published 11 Mar 2010

of GHz, a feature which is difficult to achieve either in conventional microwave phase shifters or in those based on the novel approaches previously discussed.

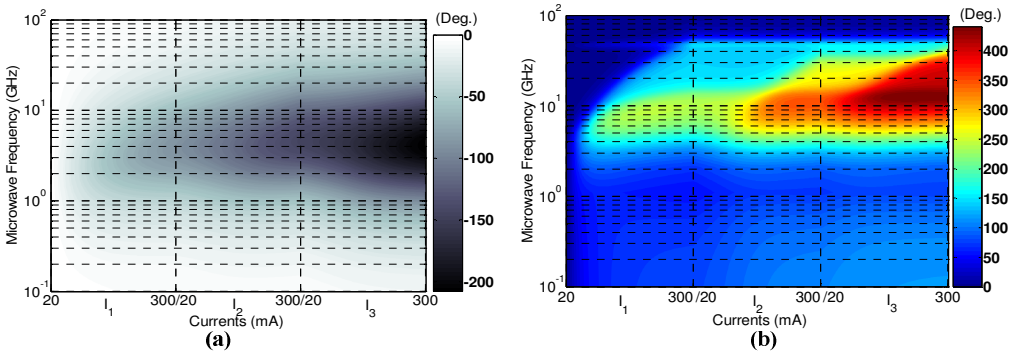


Fig. 2. Calculated microwave phase shift as a function of both microwave frequency and the injection currents of three SOAs. (a) Conventional case without optical filtering, which corresponds to simply cascading five SOAs. (b) Blocking the red-shifted sidebands.

*2.2 Experimental demonstrations*

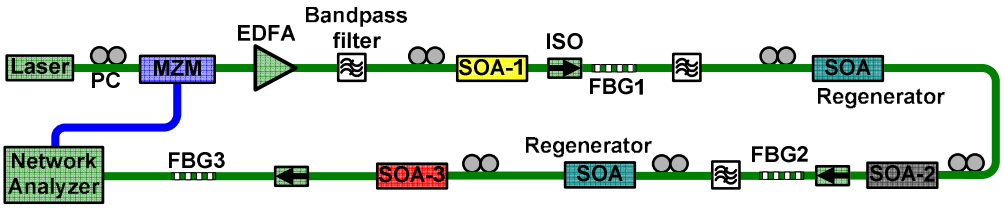


Fig. 3. Experimental set-up for measuring the microwave phase shift. (PC: polarization controller; MZM: Mach-Zehnder intensity modulator; EDFA: erbium doped fiber amplifier; ISO: fiber isolator; FBG: fiber Bragg grating). The laser at the wavelength of 1539nm is intensity modulated by the microwave electrical signal from the network analyzer, which is also used to measure the microwave phase shift induced by the SOAs.

We have experimentally investigated the suggested slow-light configuration using the set-up depicted in Fig. 3. Optical filtering, needed to block the red-shifted sideband, is accomplished using fiber Bragg grating (FBG) notch filters. Three optical bandpass filters are employed to suppress the amplified spontaneous emission noise (ASE). During the measurements, the two regeneration SOAs are biased at a fixed current. To measure the microwave phase shift induced by the proposed phase shifter in isolation, a calibration measurement has to be performed. We here take the reference point to be the situation in which the injection currents ($I_1$, $I_2$, $I_3$) equal their transparency values of (80mA, 80mA, 80mA).

Figures 4a and 4b give the measured microwave phase shifts and relative power changes at a microwave frequency of 40 GHz. When the three FBGs are included to block the red-shifted sidebands, ~130°, ~120°, and ~120° RF phase delays are achieved by increasing $I_1$, $I_2$, and $I_3$, respectively. The total 370° RF phase shift at 40 GHz verifies the scalability of the proposed scheme.

For a single phase shifter stage, the abrupt phase change is accompanied by a dip in the microwave power [15]. This might be thought to limit the cascadability, since large amplitude changes will be unacceptable for most applications. However, it was found that these microwave power dips, induced by increasing $I_1$, $I_2$, and $I_3$, respectively, decrease progressively, and the corresponding microwave phase shifts are less abrupt. This effect, which is very important for the practical scalability of the phase shifters, can be understood by considering the chirp of the optical signal acquired by the preceding SOAs. Thus, the sidebands will in general acquire slightly different phases, corresponding in the time domain

#122608 - $15.00 USD Received 12 Jan 2010; revised 22 Feb 2010; accepted 9 Mar 2010; published 11 Mar 2010

to a combination of amplitude and phase modulations, and thereby decrease the microwave power dip induced by the following SOAs. This effect was previously studied for a single SOA by considering the influence of the input chirp [28]. This interpretation is confirmed by comparison with numerical simulations, shown as black solid lines in Figs. 4a and 4b, based on a four-wave mixing model [12].

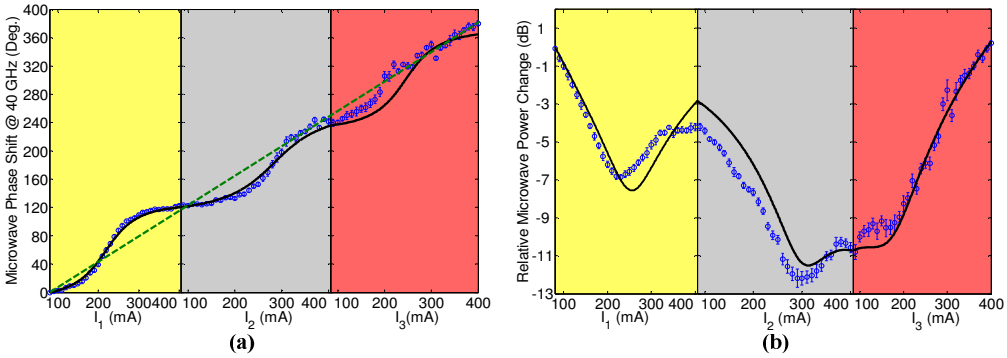


Fig. 4. Experimental demonstration of 360° microwave phase shift. (a) Microwave phase shift and (b) power changes at the microwave frequency of 40 GHz. The injection currents ($I_1$, $I_2$, $I_3$) are increased from 80 mA to 400 mA consecutively. The markers are experimental data and the black solid lines are numerical simulations. The green dashed line shows a linear fit.

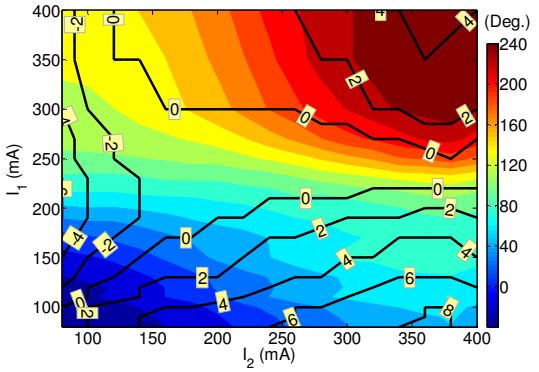


Fig. 5. Experimental demonstration of microwave phase shift (colour contour) and relative power change (black solid lines). The measurements are shown as a function of the currents $I_1$ and $I_2$ with $I_3$ being fixed at 80 mA, and performed at 40 GHz.

The introduction of several phase shift stages provides additional flexibility for tailoring the linearity of the phase shift, its frequency response as well as the variation of the corresponding amplitude by choosing different current combinations ($I_1$, $I_2$, $I_3$). Besides achieving a large absolute phase shift, these characteristics are of utmost importance for a number of applications. Figure 5 shows the measured microwave phase and power in dependence of two of the currents while keeping the third fixed. It is important to note that the contour lines of phase and power, in some regions, are near-orthogonal and in general are not parallel. This allows independent control of phase and power. As an example, by controlling the currents ($I_1$, $I_2$) to follow the 2 dB power contour line, a tunable >200° microwave phase shift at 40 GHz with less than 2 dB power fluctuation can be obtained. By controlling all three currents, 360° phase shift with minimal power variation is feasible. We notice that the need to control several currents is similar to the control problem encountered in the case of continuously tunable multi-section laser diodes.

#122608 - $15.00 USD Received 12 Jan 2010; revised 22 Feb 2010; accepted 9 Mar 2010; published 11 Mar 2010

### 3. Microwave operation bandwidth of 360° phase shifters

We have also experimentally investigated the microwave modulation frequency dependence of the proposed phase shifter. Measured results are shown in Fig. 6a for a single phase shifter stage by plotting the phase change versus power and frequency in a contour diagram. In this case, a microwave phase delay of more than 100° is obtained up to 35 GHz. We have analyzed the origin of the bandwidth enhancement of the optical filtering techniques using the four-wave mixing model. For intensity modulated signals at a modulation frequency ranging up to several hundred GHz, wave mixing is dominated by the pulsations of the carrier density. The carrier population oscillations induce wave mixing among the three electrical fields, $E_0$, $E_{-1}$, $E_{+1}$ representing the strong carrier and two weak sidebands and modify the gain and index of the sidebands. The evolution of these field components are described by three differential equations, e.g. Eq. (1) of reference [28]. The detected microwave signals, without optical filtering or considering the blocking of the red-shifted sideband can be expressed as $P_0$ ( $= E_0^* \cdot E_{+1} + E_{-1}^* \cdot E_0$) and $P_{+1}$( $= E_0^* \cdot E_{+1}$), respectively. These new variables are governed by Eq. (3) in [28] and can easily be numerically computed. To better understand the microwave phase shift, the terms only related to the amplitude of Eq. (3) in [28] can be neglected. Thus, analytical solutions of the phase of the modulated signal are achieved for the cases without optical filtering and with the red-shifted sideband blocked. In this case, however, all information regarding the amplitude of the modulated signal is lost. An approximate analytical solution is derived for the maximum microwave modulation frequency:

Without optical filtering:

$$\Omega_{\max}(S,\tau_s) = (1+S)\cdot\frac{1}{\tau_s} \tag{1}$$

Blocking the red-shifted sideband:

$$\Omega_{\max}(S,\tau_s,\alpha) = \frac{S+\sqrt{S^2-4(1+S)^4\Phi^2}}{2\Phi(1+S)}\cdot\frac{1}{\tau_s} \tag{2}$$

where $\Phi = (\pi/2 - \arctan\alpha)(/z\Gamma g_0, \Gamma g_0)$ is the linear gain, $\alpha$ is the linewidth enhancement factor, $z$ is the length of the SOA, $S$ is the input optical power normalized by the saturation power, and $\tau_s$ is the carrier recovery time. For the conventional case, where no optical filtering is performed, the microwave frequency is limited by the rate of carrier recovery, $1/\tau_s$ [12–14]. However, optical filtering is seen to enhance the available microwave frequency by a factor that depends on the power, $S$, and the linewidth enhancement factor, $\alpha$. This can be interpreted as an equalization effect brought about by the dynamics of the refractive index, not unlike the effect used in interferometers to increase the speed of all-optical signal processing [29]. In particular, by increasing $\alpha$, it is possible to significantly enhance the operating frequency. For a value of $\alpha$ of the order of 30 or more the operating frequency thus extends beyond 100 GHz. Such high $\alpha$-parameters have been realized in quantum dot active waveguides [30]. The black dashed curve in Fig. 6a is given by Eq. (2), and shows that the approximate result provides a good prediction of the microwave modulation frequency. Hence, Eq. (2) gives directions for further engineering the SOA to make it operate at a specific microwave frequency band of interest. We notice that a similar phase shift can be obtained by electrically changing the injection current of the SOA.

Expanding to the case of three cascaded stages of phase shifters, the measured frequency responses are shown in Fig. 6b. The injection currents ($I_1$, $I_2$, $I_3$) are increased, one by one, from the reference value of 80 mA to the maximum value of 400 mA. A ~360° microwave phase delay can be obtained in the entire frequency range up to 40 GHz, which is a record achievement compared to previous results both in terms of phase shift [27] and frequency range [31].

#122608 - $15.00 USD Received 12 Jan 2010; revised 22 Feb 2010; accepted 9 Mar 2010; published 11 Mar 2010

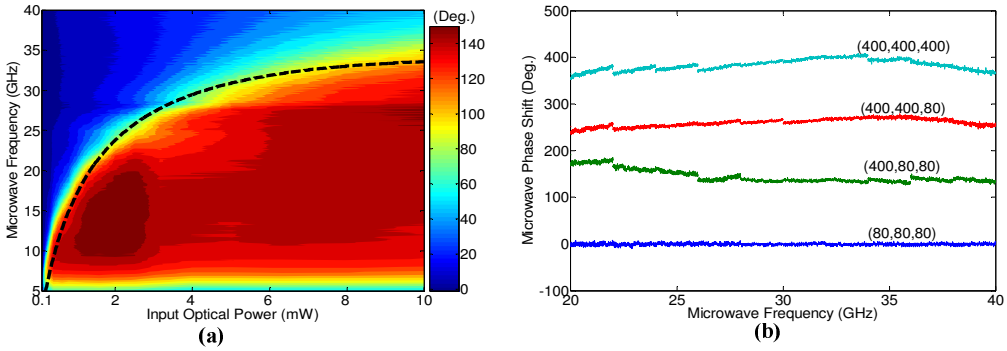


Fig. 6. Measured microwave frequency dependence of phase shifter. (a) Microwave phase shifts (colour scale) for a single phase shift stage as a function of microwave frequency and input optical power when blocking the red-shifted sideband. The black dashed curve shows the analytical result, Eq. (2). (b) Microwave phase shift for three cascaded phase shifter stages as a function of the microwave modulation frequency. The injection currents ($I_1$, $I_2$, $I_3$) are consecutively increased from 80 mA to 400 mA.

## 4. Summary and outlook

In conclusion, we have proposed a new configuration and experimentally demonstrated, for the first time, to the best of our knowledge, the realization of a tunable 360° microwave photonic phase shifter based on slow light effects in semiconductor waveguides. A >360° phase shift has been achieved in a broad frequency range up to 40 GHz, and further improvement of the bandwidth is feasible. The demonstration is based on the cascading of several semiconductor optical amplifiers, with in-between stages of optical filtering and regeneration. The phase shift and regeneration are realized using coherent population oscillations and four-wave mixing in active waveguides. The proposed phase shifter can be reconfigured on a sub-nanosecond time-scale and the operation voltage is on the order of 1 volt. The operating frequency and the bandwidth are strongly enhanced by optical filtering and we have obtained a simple analytical expression accounting for the enhancement beyond the usual limitation of the inverse lifetime, which provides directions for further engineering of the device. Finally, the suggested approach allows large flexibility in tailoring the linearity and frequency response of the system.

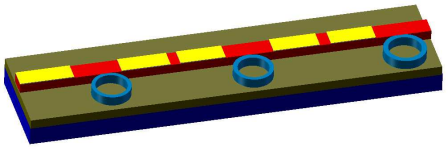

Fig. 7. Sketch of a possible monolithic implementation of a microwave photonic phase shifter with micro-rings to realize optical filtering.

Furthermore, if the optical filtering is realized monolithically, e.g. by micro-ring structures, surface gratings or Bragg filters, this scheme allows a fully integrated device. An important issue in such a design is to avoid feedback effects from the integrated filters, which could lead to lasing. Figure 7 shows a schematic of a possible implementation of such a monolithically integrated microwave photonic phase shifter. We therefore believe that the proposed method for achieving microwave photonic phase shifts will pave the way for future applications in microwave photonic systems.


## Acknowledgments

The authors would like to acknowledge support from the European Commission via the FP7 project “GOSPEL” as well as the Danish Research Councils via the project “QUEST” and the Generalitat Valenciana via project PROMETEO 2008/92.

#122608 - $15.00 USD Received 12 Jan 2010; revised 22 Feb 2010; accepted 9 Mar 2010; published 11 Mar 2010